https://doi.org/10.5194/gmd-2020-181
Preprint. Discussion started: 3 July 2020

Geoscientific Model Development Discussions

Development of WRF/CUACE v1.0 model and its preliminary application in simulating air quality in China

Lei Zhang[1], Sunling Gong[1]*, Tianliang Zhao[2]*, Chunhong Zhou[1], Yuesi Wang[3], Jiawei Li[4], Dongsheng Ji[3], Jianjun He[1], Hongli Liu[1], Ke Gui[1], Hong Wang[1], Yaqiang Wang[1], Huizheng Che[1], Xiaoye Zhang[1]

[1] State Key Laboratory of Severe Weather & Key Laboratory of Atmospheric Chemistry of CMA, Chinese Academy of Meteorological Sciences, Beijing 100081, China
[2]Climate and Weather Disasters Collaborative Innovation Center, Nanjing University of Information Science &Technology, Nanjing, 210044 China
[3]State Key Laboratory of Atmospheric Boundary Layer Physics and Atmospheric Chemistry, Institute of Atmospheric Physics, Chinese Academy of Sciences, Beijing, 100029, China
[4] CAS Key Laboratory of Regional Climate-Environment for Temperate East Asia (RCE-TEA), Institute of Atmospheric Physics, Chinese Academy of Sciences, Beijing 100029, China

Correspondence to: Sunling Gong (gongsl@cma.gov.cn) and Tianliang Zhao (tlzhao@nuist.edu.cn)

Abstract. The development of chemical transport models with advanced physics and chemical schemes could improve air-quality forecasts. In this study, the China Meteorological Administration Unified Atmospheric Chemistry Environment (CUACE) model, a comprehensive chemistry module incorporating gaseous chemistry and a size-segregated multicomponent aerosol algorithm, was coupled to the Weather Research and Forecasting (WRF)-Chem framework using an interface procedure to build the WRF/CUACE v1.0 model. The latest version of CUACE includes an updated aerosol dry deposition scheme and the introduction of heterogeneous chemical reactions on aerosol surfaces. We evaluated the WRF/CUACE v1.0 model by simulating $PM_{2.5}$, O_3, and NO_2 concentrations for January, April, July, and October (representing winter, spring, summer, and autumn, respectively) in 2013, 2015, and 2017 and comparing them with ground-based observations. Secondary inorganic aerosol simulations were also evaluated through a simulation of a heavy haze pollution event during 9–15 January 2019 in the North China Plain. The model well captured the variations of $PM_{2.5}$, O_3, and NO_2 concentrations in all seasons in eastern China. However, it is difficult to accurately reproduce the variations of air pollutants over Sichuan Basin, due to its deep basin terrain. The sulfate and nitrate simulations are substantially improved by introducing heterogenous chemical reactions into the CUACE model (change in bias from −95.0% to 4.1% for sulfate and from 124.1% to 96.0% for nitrate). The development of the WRF/CUACE v1.0 model represents an important step towards improving air-quality modelling and forecasts in China.

1 Introduction

The atmosphere is an extremely complex reaction system in which a large number of chemical and physical processes occur at every moment. Numerical modelling has become an effective means to

https://doi.org/10.5194/gmd-2020-181
Preprint. Discussion started: 3 July 2020


Geoscientific Model Development Discussions
Open Access
EGU

study atmospheric environmental changes and their mechanisms due to its capability at large spatial-temporal scales and with high resolution. Against the continuing rapid increase in fine particle pollution in China, chemical transport models (CTMs) have been developed in recent years and new physical and chemical atmospheric mechanisms have been presented, for instance, heterogenous chemical reactions, the production of secondary organic and inorganic aerosols, and dry deposition schemes. However, some of the mechanisms have yet to be well parameterized into CTMs for air-quality forecasts in China. Numerical modelling in combination with field observations and laboratory analyses is constantly improving our understanding of atmospheric physical and chemical processes. There is an urgent need to develop and improve CTMs to provide more powerful tools for studying the atmospheric environment, in particular for the mitigation of fine particle pollution in China.

Meteorological conditions is accepted as one of the main factors affecting atmospheric chemical processes and the aerial transport of noxious materials, and, in turn, chemical species can impact meteorological conditions by radiation feedback and cloud formation (Grell and Baklanov, 2011). Historically, CTMs were developed separately from meteorological models owing to the complexity of the atmosphere and the economics of computer calculations. Thus, CTMs were generally driven by meteorological datasets from a pre-run of the meteorological model. Information about the rapid meteorological processes, such as changes in wind direction and speed or the planetary boundary layer, are barely recorded by the low-temporal-resolution meteorological outputs (typically once or twice per hour), which may impact the accuracy of the air-quality forecasts. Coupled systems that realize the synchronous integration and two-way interactions of meteorology and chemistry are an important development for the traditional CTM approach to air-quality forecasting and there have been many endeavors devoted to this (Jacobson et al., 1996; Lin et al., 2020; Lu et al., 2020; Zhang et al., 2010).

To tackle serious air pollution in China and East Asia, with a particular focus on haze pollution forecasting, the China Meteorological Administration (CMA) has been developing the Chinese Unified Atmospheric Chemistry Environment (CUACE) model, a chemistry module that can be driven by meteorological models. The CUACE has been integrated into the Fifth-Generation Penn State/NCAR Mesoscale Model (MM5) and the mesoscale version of the Global/Regional Assimilation and Prediction System (GRAPES, a meteorological model developed by CMA) to build a fog-haze forecasting system (An et al., 2016; Wang et al., 2015a; Zhou et al., 2012). Both of these coupled systems have been running operationally at national and provincial meteorological administrations since 2014, and have been used for air-quality assurance for many major events in China. However, active development of the MM5 model ended with version 3.7.2 in 2005, and it has

https://doi.org/10.5194/gmd-2020-181
Preprint. Discussion started: 3 July 2020


Geoscientific Model Development Discussions

been largely superseded by the Weather Research and Forecasting (WRF) model. The WRF model has been shown to have a better performance relative to the MM5 model due to its better numerical dynamic core and greater number of physical parameterization schemes, and it is now used as a host model for coupling with different CTMs for scientific research and air-quality forecasting, such as the WRF-Chem and WRF-CMAQ models (Grell et al., 2005; Wong et al., 2012). The WRF model has also been used to provide pre-run meteorological fields to drive models such as CAMx and FLEXPART, as well as to provide boundary and initial fields for local-scale models. Therefore, it is important to develop the CUACE module by coupling it with state-of-the-art meteorological models.

The chemical reaction mechanisms in the CUACE module, as well as in current CTMs, are proposed under clean conditions. In the context of composite air pollution in China, particularly during severe haze episodes with a rapid increase in fine particles ($PM_{2.5}$), their applicability needs to be improved. Heterogenous chemical reactions, mechanisms missing in current models, were revealed as a crucial factor to explain the dramatic increase of $PM_{2.5}$ during hazy days (Zheng et al., 2015), such as the heterogenous uptake of dinitrogen pentoxide at night (Wang et al., 2017), and the heterogeneous oxidation of dissolved SO_2 by NO_2 (Gao et al., 2016; Seinfeld and Pandis, 2012). Another process focused on here is the dry deposition of particles, where the difference between model predictions and field measurements appears greatest for vegetated canopies and for the accumulation size range of airborne particles. Ongoing research is investigating the factors that give rise to this discrepancy and providing new approaches to predicting the deposition (Hicks et al., 2016). However, few studies have incorporated these mechanisms into 3D CTMs (Wu et al., 2018).

The objectives of this study were to develop the CUACE module from three aspects: (1) introduce heterogenous reactions and update the dry deposition scheme of particles; (2) couple the CUACE to the WRF model to build the WRF/CUACE v1.0 system; and (3) evaluate the model against observations of surface air pollutants.

2 Model description

2.1 WRF model

The Advanced Research WRF version 3 (WRF-ARW) is used to simulate meteorological processes and advection of atmospheric components in the WRF/CUACE v1.0 model. The WRF-ARW is a state-of-the-science mesoscale meteorological model, making simulations that are based on actual atmospheric conditions or idealized conditions feasible (Langkamp and Böhner, 2011). The equation set for the WRF-ARW is fully compressible, Eulerian non-hydrostatic with a run-time

https://doi.org/10.5194/gmd-2020-181
Preprint. Discussion started: 3 July 2020


Geoscientific Model Development Discussions

hydrostatic option. It is conservative for scalar variables. The prognostic variables consist of velocity components *u* and *v* in Cartesian coordinates, vertical velocity *w*, perturbation potential temperature, perturbation geopotential, and perturbation surface pressure of dry air, as well as several optional prognostic variables depending on the model physical options (Skamarock et al., 2008; Wong et al., 2012).

2.2 CUACE module

The CUACE module is a unified atmospheric chemistry module incorporating three major functional modules: emissions, gaseous chemistry, and a size-segregated multicomponent aerosol algorithm (Zhou et al., 2012), and has been designed as a unified chemistry module that can be coupled to any atmospheric model at various temporal and spatial scales. The CUACE is typically configured with the second generation of the Regional Acid Deposition Model (RADM2) as its gaseous chemistry module, which represents 63 species through 21 photochemical reactions and 121 gas phase reactions. The Canadian Aerosol Module (CAM) (Gong et al., 2003) is adopted as its aerosol module. There are seven types of aerosols treated in CAM, i.e. black carbon, organic carbon, sulfates, nitrates, ammonium, soil dust, and sea salts. The sea salt emissions are calculated online using the parametrization scheme developed by Gong et al. (2003). Soil dust emissions are simulated using the Marticorena–Bergametti–Alfaro scheme (Alfaro and Gomes, 2001; Marticorena and Bergametti, 1995). With the exception of ammonium, the aerosol size spectrum is divided into 12 bins with fixed boundaries of 0.005–0.01, 0.01-–0.02, 0.02–0.04, 0.04–0.08, 0.08–0.16, 0.16–0.32, 0.32–0.64, 0.64–1.28, 1.28–2.56, 2.56–5.12, 5.12–10.24, and 10.24–20.48 μm. The multicomponent aerosols in each size bin are subject to the mass conservation equation as follows:

$$\frac{\partial X_{ip}}{\partial t} = \frac{\partial X_{ip}}{\partial t}\Big|_{TRANSPORT} + \frac{\partial X_{ip}}{\partial t}\Big|_{SOURCES} + \frac{\partial X_{ip}}{\partial t}\Big|_{CLEARAIR} + \frac{\partial X_{ip}}{\partial t}\Big|_{DRY} + \frac{\partial X_{ip}}{\partial t}\Big|_{IN-CLOUD} + \frac{\partial X_{ip}}{\partial t}\Big|_{BELOW-CLOUD} ,$$

where the change rate in the mixing ratio of dry particle mass constituent p within the size range i has been divided into components (or tendencies) for transport, sources, clear air, dry deposition, and in-cloud and below-cloud processes. The main aerosol processes considered in CAM include coagulation, nucleation, condensation, collision, aerosol-cloud interaction, dry deposition, and wet scavenging (An et al., 2016; Gong et al., 2003).

3 Development of the CUACE module

3.1 Update with particle dry deposition scheme

The CUACE module currently parameterizes particle dry deposition velocity according to the

https://doi.org/10.5194/gmd-2020-181
Preprint. Discussion started: 3 July 2020


Geoscientific Model Development Discussions

method of Zhang et al. (2001) (Z01), which tends to overestimate the dry deposition, especially for fine particles (Petroff and Zhang, 2010). In this study, we use the scheme that developed by Petroff and Zhang (2010) (PZ10) to replace the original scheme in the CUACE module. Both schemes use the "resistance" analogy, but with quite different formulas. The PZ10 scheme improved the surface resistance and collection efficiency of the Z01 scheme to overcome the problem of overestimating the dry deposition velocity of fine particles. The PZ10 scheme is detailed as follows:

$$V_d = V_{drift} + \frac{1}{R_a + R_s} \quad (1)$$

Here V_{drift} represents drift velocity, which is equal to the sum of gravitational settling and phoretic velocity and is expressed as

$$V_{drift} = V_g + V_{phor} \quad (2)$$

where V_g is the gravitational settling velocity and V_{phor} accounts for the phoretic effects that are related to differences in temperature, water vapor, or electricity between the collecting surfaces and the air.

The aerodynamic resistance (R_a) and surface resistance (R_s) are calculated differently for vegetated and unvegetated surfaces. For vegetated surfaces, R_a is parameterized as

$$R_a = \frac{1}{\kappa u_*}\left[\ln\left(\frac{z_R - d}{h - d}\right) - \Psi_h\left(\frac{z_R - d}{L_O}\right) + \Psi_h\left(\frac{h - d}{L_O}\right)\right] \quad (3)$$

where κ is the von Karman constant (0.4), u_* is the friction velocity above canopy, z_R is the reference height, h is the canopy height, d is the displacement height of the canopy, L_O is the Obhukov length, and Ψ_h is the integrated form of the stability function for heat.

Surface resistance (R_s) is generally expressed as the reciprocal of the surface deposition velocity (V_{ds}), which is parameterized as

$$V_{ds} = u_* E_g \frac{1 + \left[\frac{Q}{Q_g} - \frac{\alpha}{2}\right]\frac{\tan h\eta}{\eta}}{1 + \left[\frac{Q}{Q_g} + \alpha\right]\frac{\tan h\eta}{\eta}} \quad (4)$$

where E_g is the total collection efficiency on the ground below the vegetation and consists of two parts: (1) Brownian diffusion (E_{gb}) and (2) turbulent impaction (E_{gt}). E_{gb} is parameterized as

$$E_{gb} = \frac{Sc^{-\frac{2}{3}}}{14.5}\left[\frac{1}{6} ln \frac{(1+F)^2}{1-F+F^2} + \frac{1}{\sqrt{3}} Arctan \frac{2F-1}{\sqrt{3}} + \frac{\pi}{6\sqrt{3}}\right]^{-1} \quad (5)$$

where F is a function of the Schmidt number (S_c) and is parameterized as $F = Sc^{\frac{1}{3}}/2.9$. E_{gt} is expressed as

$$E_{gt} = 2.5 \times 10^{-3} C_{IT} \tau_{p\hbar}^{+2}, \quad (6)$$

where C_{IT} is a constant taken as 0.14 and $\tau_{p\hbar}^{+}$ is a function of non-dimensional relaxation time of

https://doi.org/10.5194/gmd-2020-181
Preprint. Discussion started: 3 July 2020


Geoscientific Model Development Discussions

the particle.

In equation (4), the non-dimensional timescale parameter, Q, represents the ratio of turbulent transport timescale to vegetation collection timescale, and Q_g is the analogy of Q used for the transfer to the ground. Q << 1 characterizes a situation where turbulent mixing is efficient and the transfer of particles is limited by the collection efficiency on leaves. Meanwhile, Q >>1 corresponds to a situation where particles are efficiently collected by leaves and transfer of turbulent mixing is limited. Q and Q_g are defined as:

$$Q = \frac{LAI E_T h}{l_{mp}(h)} \quad (7)$$

$$Q_g = \frac{E_g h}{l_{mp}(h)} \quad (8)$$

where LAI is the two-sided leaf area index, E_T is the total collection efficiency by various physical processes, and l_{mp} is the mixing length for particles. E_T is expressed as:

$$E_T = \frac{U_h}{u_*}(E_B + E_{IN} + E_{IM}) + E_{IT} \quad (9)$$

where U_h is the horizontal mean wind speed at canopy height h; and E_{B}, E_{IN}, E_{IM}, and E_{IT} are the collection efficiencies by Brownian diffusion, interception, inertial impaction, and turbulent impaction, respectively. The term η is taken as

$$\eta = \sqrt{\frac{\alpha^2}{4}} + Q \quad (10)$$

where α is the aerodynamic extinction coefficient, and is expressed as

$$\alpha = \left(\frac{k_x LAI}{12k^2\left(1-\frac{d}{h}\right)^2}\right)^{\frac{1}{3}} \phi_m^{\frac{2}{3}}\left(\frac{h-d}{L_O}\right) \quad (11)$$

where k_x is the inclination coefficient of the canopy elements and ϕ_{m} is the non-dimensional stability function for momentum.

For non-vegetated surfaces, the aerodynamic resistance Ra is calculated as

$$Ra = \frac{1}{\kappa u*}\left[\ln\left(\frac{z_R-d}{z_0}\right) - \Psi_h\left(\frac{z_R-d}{L_O}\right) + \Psi_h\left(\frac{z_0}{L_O}\right)\right] \quad (12)$$

and the surface deposition velocity V_{ds} is expressed as

$$V_{ds} = u_*(E_{gb} + E_{IT}) \quad (13)$$

3.2 Introduction of heterogeneous chemistry

The study of heterogeneous chemical reactions mostly focuses on the surface of dust aerosols, but the parameterization schemes of heterogeneous chemical reactions on different types of aerosol have not been well established (Zheng et al., 2015). The following are the heterogeneous chemical

https://doi.org/10.5194/gmd-2020-181
Preprint. Discussion started: 3 July 2020

Geoscientific Model Development Discussions

reactions on aerosol surfaces that added to the CUACE module in this study:

H_2O_2 (gas) + Aerosol → Products （14）

HNO_3 (gas) + Aerosol → $0.5NO_3^-$ + $0.5NO_x$ (gas) （15）

HO_2 (gas) + Fe(II) → Fe(III) + H_2O_2 （16）

N_2O_5 (gas) + Aerosol → $2\ NO_3^-$ （17）

NO_2 (gas) + Aerosol → NO_3^- （18）

NO_3 (gas) + Aerosol → NO_3^- （19）

O_3 (gas) + Aerosol → Products （20）

OH (gas) + Aerosol → Products （21）

SO_2 (gas) + Aerosol → SO_3^- （22）

Reactions (15) and (17)–(19) describe the formation of sulfate and nitrate on the surface of sand dust, and the other four reactions describe mineral aerosols as sinks of gaseous substances. In this study, these nine heterogeneous reactions were extended to all types of aerosol surface in the CUACE, referring to the approach of Zheng et al. (2015) for the CMAQ model. The first-order chemical kinetic equation for calculating the adsorption efficiency of a gas on an aerosol surface is:

$$\frac{dC_i}{dt} = -k_i C_i \quad (23)$$

where C_i represents the concentration of gas i and k_i is the pseudo-first-order rate constant and is supposed to be irreversible. The value of k_i is defined referring to Jacob (2000) as:

$$k_i = \left(\frac{a}{D_i} + \frac{4}{v_i \gamma_i}\right)^{-1} A \quad (24)$$

where a is the aerosol diameter, D_i is the diffusion coefficient for gas reactant i, v_i is the mean molecule speed of gas reactant i, γ_i is the uptake coefficient of the heterogeneous reaction for the gas reactant i, and A is the surface area of aerosols in unit volume air. The value of γ_i is obtained from previous laboratory studies (Table 1) and other parameters are calculated in the WRF/CUACE v1.0 model.

4 Coupling of the CUACE module with the WRF model

The coupling of the WRF/CUACE v1.0 model uses most of the existing infrastructure in the WRF-Chem model. Following the registry tools for automatic generation of application code in the WRF-Chem model, a registry file (registry.cuace) is written to store the chemical variables of the CUACE module, as well as a new parameter of chem_opt (122) for users to start the WRF/CUACE v1.0 model. An interface procedure, cuace_driver, was first designed to integrate the core sections of the aerosol physical and chemical processes in the CUACE module (module_ae_cam.F) with the WRF framework. The interface procedure is placed in the chemical interface of WRF-Chem (chem_driver). As the gas-phase chemistry (RADM2) in the CUACE model is not computationally economic and it is hard coded, which means that it is not conducive to adapting chemical reactions in

https://doi.org/10.5194/gmd-2020-181
Preprint. Discussion started: 3 July 2020


Geoscientific Model Development Discussions

the future, the CBM-Z gas chemistry mechanism with a better computational efficiency is added with the KPP (Kinetic PreProcessor) protocol as the gas chemistry mechanism of the CUACE module.

The flow of the major process splitting in the coupled WRF/CUACE v1.0 model is illustrated in Fig. 1. Process splitting in the WRF/CUACE v1.0 model is generally the same as in the WRF-Chem model. The CUACE module is independent from the original chemical module of WRF-Chem, except that they share the same advective/convective transport scheme, anthropogenic emissions module, and the dry/wet deposition of gas species. In the CUACE module, most of the aerosol physical and chemical processes, such as coring, collision, condensation, dry deposition, wet scavenging, and aerosol activation, are gathered to the CAM section (Fig. 1). Meteorological fields outputted from the WRF model and chemical species from the CUACE module can exchange directly through the interface procedure. No spatial interpolation of the meteorological and chemical data is required as both the CUACE and the WRF models can be configured to the same gird configurations and coordinate systems. The feedback of chemical species on meteorology in the current WRF/CUACE version is not realized, but is under development and will be released in a future paper.

5 Performance of WRF/CUACE v1.0 in air-quality simulation

5.1 Model configuration

At present, there are four major polluted areas in China, namely, the North China Plain (NCP), the Yangtze River Delta (YRD), the Pearl River Delta (PRD), and Sichuan Basin (SCB). To include all these regions, the simulation area is configured as in Fig. 2. There are two domains in total. The boundary field of the inner domain is obtained by the interpolation of its outer domain. The outer region covers the whole of East Asia and its adjacent areas with a horizontal resolution of 54 km and a total of 120×110 grids centered at 30.46° N and 105.82° E. The inner region covers most of China on the east side of the Qinghai-Tibet Plateau with a horizontal resolution of 18 km and 193×175 grids. There are 32 vertical layers with the top pressure at about 100 hPa. The main physical and chemical options in the model are shown in Table 2. We performed two simulations. One for January, April, July, and October in three years, 2013, 2015, and 2017, to evaluate the model on a long timescale, and one for 5–16 January 2019, during which intensive observations of secondary inorganic aerosols (SIA) were performed at Xianghe Site (39.798°N, 116.958°E; 15 m above sea level), which is approximately 35 km northeast of Langfang city (Fig. 2) in the NCP region, to investigate improvements in simulating SIA with heterogenous chemistry.

https://doi.org/10.5194/gmd-2020-181
Preprint. Discussion started: 3 July 2020

The model uses the FNL global reanalysis data of the NCEP (National Centers for Environmental Prediction) to provide the meteorological initial and boundary fields with spatial and temporal resolution of 6 h and 1°×1°, respectively. The initial and boundary chemistry conditions are based on the vertical profiles of O_3, SO_2, NO_2, VOCs (volatile organic compounds), and other air pollutants from the NOAA Aeronomy Lab Regional Oxidant Model (NALROM) (Liu et al., 1996).

Anthropogenic emissions are derived from the MIX emission inventory (http://www.meicmodel.org/dataset-mix.html) (Li et al., 2017), which is an Asian anthropogenic emissions inventory developed for the third phase of the East Asian Model Comparison Plan (MICS-Asia III) and the United Nations Hemispheric Atmospheric Pollution Transport Plan (HTAP). The inventory provides monthly grid emission data with 0.25° spatial resolution for five emission sectors (electricity, industry, civil, transportation, and agriculture), including $PM_{2.5}$, PM_{10}, nitrogen oxides (NO_x), sulfur dioxide (SO_2), carbon monoxide (CO), NH_3, black carbon (BC), organic carbon (OC), and non-methane volatile organic compounds (NMVOCs). During the simulation span from 2013 to 2017, China carried out strict air pollution control measures, which had a considerable impact on anthropogenic emissions. To make the anthropogenic emissions more suitable for the real emissions scenarios in the simulated years, the emissions in mainland China were replaced with the MEIC emissions inventory in 2012, 2014, and 2016 to represent the emissions scenarios of mainland China in 2013, 2015, and 2017, respectively.

For the vertical interpolation, we used the settings of Wang et al. (2010) and Zhou et al. (2017). The industrial emissions were allocated as 50, 30, and 20% in layers one to three of the model, respectively, and the power plant emission sources were allocated as 14, 46, 35, and 5% in model layers two to five, respectively. The emissions from transportation, residential, and agriculture were 95% and 5%, respectively, in the first and second layers of the model. Then, the inventory was distributed into hourly emissions using the monthly, weekly, and hourly profiles established by Tsinghua University (2006). VOCs released from vegetation was calculated online using the MEGAN model (Guenther, 2006).

5.2 Evaluation against ground-based observations

In view of the spatial-temporal differences in the haze pollution that occur in the four different regions (i.e. NCP, YRD, PRD, and SCB), here we assessed surface $PM_{2.5}$, O_3, and NO_2 simulated in the WRF/CUACE v1.0 model by region and season. Figure 3 presents a comparison of the modelled and observed daily mean $PM_{2.5}$ concentrations in spring, summer, autumn, and winter in the four regions. Overall, the WRF/CUACE v1.0 model well captured the variations in the $PM_{2.5}$

https://doi.org/10.5194/gmd-2020-181
Preprint. Discussion started: 3 July 2020

concentration, but with different performance in different regions and seasons. The correlation coefficients (*R*) for the NCP, YRD, and PRD are mostly above 0.60 and passed the 99% significance test. The *R* value between the YRD and PRD is the highest (generally higher than 0.65), followed by the NCP. The NCP, YRD, and SCB simulations in autumn and winter are generally better than that in spring and summer according to the *R* values, while that in the PRD is the opposite with a better performance during spring and summer seasons. The simulations are relatively poor in the SCB, where the complex terrain poses great challenges to meteorological field simulations.

It is noteworthy that the WRF/CUACE v1.0 model systematically underestimated the daily $PM_{2.5}$ concentrations in the NCP when it exceeded about 200 μg m^{-3}, which mostly happened during winter (Fig. 4a). By comparing the time series of observations and simulations, we found that the underestimation mainly occurred in the period of heavy haze pollution in some cities (such as Shijiazhuang, Hengshui, Handan, etc.). Two factors might be responsible for this. One is the uncertainty of emission sources. The formulation of an accurate emissions source inventory is always a difficult problem, especially in China. In the NCP, the seasonal difference in emission sources is substantial. A large number of unorganized loose coal combustion emissions during the winter heating season cannot be promptly accounted for by the emissions source inventory system, which increases the uncertainty of the local emission sources. The other factor might be problems in the chemical reaction mechanisms. The haze pollution study found that $PM_{2.5}$ was mainly composed of secondary particulate matter, including sulfate, nitrate, ammonium salt, and SOA. During heavy haze episodes, the concentration of sulfate increased substantially, but its formation mechanism remains not well recognized. The main international atmospheric chemical models (such as CMAQ, WRF-Chem, CAMx, etc.) are also found to be not ideal enough to simulate sulfate and SOA during heavy haze pollution in North China. Zheng et al. (2015) and Gao et al. (2016) initially added SO_2 heterogeneous processes in the CMAQ and WRF-Chem models, and the simulation results of sulfate improved. Although heterogeneous chemical reaction mechanisms are introduced in this study, the simulation effect of sulfate needs to be further evaluated, and the simulation of SOA is more challenging, involving thousands of VOC species and determination of their saturation, atmospheric oxidation, free radicals, acidity, and basicity. The development of a volatility basis set (VBS) is a major breakthrough that treats the organic gas/particle partitioning with a spectrum of volatilities using a saturation vapor concentration as the surrogate of volatility (Ahmadov et al., 2012; Donahue et al., 2006; Wang et al., 2015b).

The WRF/CUACE v1.0 model was further evaluated using hourly $PM_{2.5}$ concentrations and *R*, mean bias (MB), mean error (ME), normalized mean bias (NMB), normalized mean error (NME), mean fractional bias (MFB), and mean fractional error (MFE) (Table 3). As can be seen from Table

https://doi.org/10.5194/gmd-2020-181
Preprint. Discussion started: 3 July 2020


Geoscientific Model Development Discussions

3, the correlation coefficients *R* for the NCP, YRD, PRD, and SCB are 0.59, 0.71, 0.68, and 0.59, respectively, all of which passed the 99% significance test. The YRD has the best correlation, followed by the PRD. MB values reflect that the performance of the model is reasonable in all regions, among which those in NCP and PRD are the best, with the MB values reaching −5.0 and 5.3 ug m^{-3}, respectively. However, the MB values show that the simulated concentration of $PM_{2.5}$ in NCP during winter is generally underestimated by 45 ug m^{-3}.

From the point of view of relative deviation, the overall level of standard mean deviation NMB in the NCP is slightly better than that in the YRD and PRD, but the seasonal difference is significant, and the NMB values of the latter two (especially in the PRD) are more uniform in different seasons, maintaining at about 20%, indicating that the simulation level of the model is relatively stable in the region. The NMB of SCB is 12.2%, which is similar to that of NCP with a significant seasonal difference (11.5% in winter and 60.4% in summer). The NMBs in the NCP, YRD and PRD are basically the same, about 45%, slightly better than 50.3% in SCB.

Morris et al. (2005) provided a reference standard for MFB and MFE using hourly concentrations of simulated and observed $PM_{2.5}$. The simulation performance is identified to be excellent when MFB < 15% and MFE < 35%, identified to be good when MFB < 30% and MFE < 50%, and identified to be average when MFB < 60% and MFE < 75%, which are marked as bold, normal, and italic font, respectively, in Table 3. It can be seen that simulations in the YRD and PRD fall within the good level with the MFB/MFE reaching 21.1/42.9% and 8.6/40.1%, respectively. Both reached excellent levels in winter, which are 8.5/34.1% and 5.5/34.4%. respectively, indicating that the WRF/CUACE v1.0 model accurately captures the hourly variations of $PM_{2.5}$ in the two regions. In the NCP region, the model still maintains a good simulation level (3.3/49.1%) in the area, with obvious overestimates in summer but still maintaining an average level (44.9/56.3%). The SCB region as a whole is at the average level (20.7/51.4%). The simulation of winter and spring is better than that of spring and summer. The reason why the simulation in SCB is relatively poor is that its topography is complex, which leads to inaccurate simulation of meteorological fields and further affects the simulation of chemical species. In addition, the uncertainty of emission sources over there is also a major factor (Zhang et al., 2019).

As a whole, the seven statistical error indicators *R*, MB, ME, NMB, NME, MFB, and MFE in the four regions reached 0.63 (99% significance test), 2.7 ug m^{-3}, 33.3 ug m^{-3}, 2.8 %, 46.8 %, 10.6 %, and 46.2%, respectively, which showed that the WRF/CUACE v1.0 model can reasonably reproduce the changes in $PM_{2.5}$.

Statistical metrics for O_3 and NO_2, including index of agreement (IOA), NMB, and *R*, are shown in Table 4, along with a benchmark derived from the EPA (2005, 2007). In general, the *R*

https://doi.org/10.5194/gmd-2020-181
Preprint. Discussion started: 3 July 2020


Geoscientific Model Development Discussions

values of O_3 and NO_2 in the four regions are about 0.6, which pass the 99% significance test. For O_3, NMBs indicate that the concentrations in the NCP, YRD, and PRD were well reproduced by simulations. The high consistency of the time series between the simulations and measurements was also reflected by the high values of IOA (>0.8). It should be noted that the NMB indicates that the O_3 concentrations in SCB were overestimated, which is also reflected in the scatter plot (Fig. 4). The complex topography and uncertainties in the emissions inventory might be responsible. As the precursor of O_3, simulation of NO_2 over the NCP, YRD, PRD, and SCB was acceptable, with the NMBs all falling within the benchmark and IOAs greater than 0.70. In general, the statistical metrics for O_3 and NO_2 are comparable with other studies (Gao et al., 2018; Hu et al., 2016).

On the basis of the above analysis results, the simulation results are satisfactory, with the exception of SCB.

5.3 Evaluation of SIA simulations with heterogeneous chemical reactions

Heterogeneous chemical reactions have been shown to have important effects on the formation of SIAs, especially during severe haze events with high humidity (Li et al., 2011; Wang et al., 2006; Zhao et al., 2013). Following the model configurations in Section 4.2, we performed WRF/CUACE v1.0 simulations with (Exp_WH) and without (Exp_WoH) heterogenous chemistry for a severe haze event that occurred on 9–15 January 2019. Figure 5 illustrates the hourly variations of observed SIA concentration from the Exp_WH and Exp_WoH experiments. The simulation without heterogenous chemistry (Exp_WoH) barely capture the sulfate increase. This was substantially improved when heterogenous chemistry was included (Exp_WH), although some observed peak values are not well captured, such as those on 14 January. The overestimation of nitrate was also improved, with the NMBs changing from 124.1% to 96.0%. It should be noted that the responses of sulfate and nitrate to heterogenous chemistry are inverse, which might be attributed to the complex thermodynamic processes of SIA formation (Zheng et al., 2015). Sulfate and nitrate will compete for ammonium, which is now the only cation currently in the CUACE model, resulting in less ammonium nitrate and more ammonium sulfate because of the more thermodynamically stable features of ammonium sulfate. As a result of the dramatical increase in sulfate in Exp_WH, the ammonium concentrations slightly increase relative to that in Exp_WoH to achieve anion–cation balance, which leads to more overestimations in the Exp_WH experiment.

6 Summary and future work

This study develops the chemical module CUACE by adding heterogenous chemical reactions

https://doi.org/10.5194/gmd-2020-181
Preprint. Discussion started: 3 July 2020

and introducing a particle dry deposition scheme developed by Petroff and Zhang (2010). The CUACE module is then incorporated into the WRF-Chem model to build the WRF/CUACE v1.0 modelling system to take advantage of the better numerical dynamic core and the greater number of physical parameterization schemes of the WRF model compared with the MM5 model.

We perform a three-year (2013, 2015, and 2017) model simulation using the WRF/CUACE v1.0 model to evaluate its performance on reproducing surface concentration variations of $PM_{2.5}$, O_3, and NO_2, which are now the main pollutants in China. A heavy haze pollution event that occurred during 9–15 January 2019 in the NCP is also selected to evaluate the SIA simulations compared with intensive ground SIA observations. The results show that WRF/CUACE v1.0 can well capture the daily and hourly variations of $PM_{2.5}$, especially in the YRD and PRD regions throughout the three years. For the NCP in winter, observed high concentrations larger than 200 μg m^{-3} are not well reproduced, which might be mainly due to uncertainties in the emissions inventory and the lack of some chemical reactions in the model. For NO_2 and O_3, the model shows small biases in the NCP, YRD, and PRD regions with correlation coefficients all larger than 0.60 and the NMBs all fall within the EPA benchmark (2005, 2007). The model shows relatively notable biases in the SCB region compared with the NCP, YRD, and PRD regions for the three pollutants, which may be mainly due to the complex terrain in the SCB (Zhang et al., 2019) and insufficient meteorological data available for the region for assimilation in the NCEP-FNL reanalysis data. The Exp_WH experiment significantly improves the hourly variations in the sulfate concentration, implying a notable contribution of heterogenous chemistry to heavy haze pollution in the NCP region. Nitrate formation is restricted in the Exp_WH experiment due to the drastic increase in sulfate, which will compete for ammonium with the nitrate. However, large uncertainties remain in the mechanisms of the heterogenous chemical reactions in the model, such as the determination of the uptake coefficients, which is based on previous studies on dust surfaces.

There are still several limitations in the current version of the WRF/CUACE v1.0 model that need to be addressed in future development. The feedback of particles, which can be divided into direct and indirect effects, is recognized to be crucial in online coupled models, especially during periods with high particle loading. Currently in the WRF-Chem model, the direct effects of aerosols are processed following the methodology described by Ghan et al. (2001). Our future work will first focus on implementing the direct effects of aerosols, i.e. radiation feedback, following the Mie calculation to realize the direct aerosol forcing. The second step is to implement the VBS scheme to add the missing processes of SOA, which has been implied to be a main cause in the underestimation of OA formation (Gao et al., 2017; Heald et al., 2005; Spracklen et al., 2011). Although the original particle dry deposition scheme is updated with that developed by Petroff and Zhang (2010), it is

https://doi.org/10.5194/gmd-2020-181
Preprint. Discussion started: 3 July 2020

difficult to evaluate whether the dry deposition process is improved as the limited technology of dry deposition observations restricts direct observations of particle dry deposition. With regards to particle dry deposition, our aim is to implement several schemes in the CUACE module, such as the schemes developed by Zhang and He (2014), Zhang and Shao (2014), and Kouznetsov and Sofiev (2012), to evaluate uncertainties in the schemes on aerosol simulation, which might help the development of the particle dry deposition scheme.

Code availability

The WRF/CUACE v1.0 model is open-source and can be accessed at a DOI repository https://doi.org/10.5281/zenodo.3872620. All source code and data can also be accessed by contacting the corresponding authors Sunling Gong (gongsl@cma.gov.cn) and Tianliang Zhao (tlzhao@nuist.edu.cn).

Competing interests

The authors declare no competing interests.

Author Contributions

Sunling Gong, Tianliang Zhao, Hong Wang, Huizheng Che and Xiaoye Zhang led the project. Lei Zhang, Sunling Gong, Chunhong Zhou and Hongli Liu developed the model code, with assistance from Jiawei Li, Jianjun He, Ke Gui and Yaqiang Wang. Lei Zhang performed the simulations and wrote the manuscript with suggestions from all authors. Yuesi Wang and Dongsheng Ji provided the data of secondary inorganic aerosols. All authors contributed to the discussion and improvement of the manuscript.

Acknowledgements

This work is supported by the National Key Foundation Study Developing Programs (No. 2019YFC0214601), National Natural Science Foundation of China (No. 91744209, 41975131, 41705080), and the CAMS Basis Research Project (No. 2020Y001). We gratefully acknowledge the Atmosphere Sub-Center of Chinese Ecosystem Research Network (SCAS-CERN) for providing the data of secondary inorganic aerosols, and thank Prof. Leiming Zhang (Air Quality Research Division, Science and Technology Branch, Environment Canada) for sharing the code of aerosol dry deposition scheme.

References

https://doi.org/10.5194/gmd-2020-181
Preprint. Discussion started: 3 July 2020

Ahmadov, R., McKeen, S., Robinson, A., Bahreini, R., Middlebrook, A., De Gouw, J., Meagher, J., Hsie, E. Y., Edgerton, E., and Shaw, S.: A volatility basis set model for summertime secondary organic aerosols over the eastern United States in 2006, Journal of Geophysical Research: Atmospheres, 117, 2012.

Alfaro, S. C. and Gomes, L.: Modeling mineral aerosol production by wind erosion: Emission intensities and aerosol size distributions in source areas, Journal of Geophysical Research: Atmospheres, 106, 18075-18084, 2001.

An, X. Q., Zhai, S. X., Jin, M., Gong, S., and Wang, Y.: Development of an adjoint model of GRAPES–CUACE and its application in tracking influential haze source areas in north China, Geoscientific Model Development, 9, 2153-2165, 2016.

Bian, H. and Zender, C. S.: Mineral dust and global tropospheric chemistry: Relative roles of photolysis and heterogeneous uptake, Journal of Geophysical Research: Atmospheres, 108, 2003.

Chen, F. and Dudhia, J.: Coupling an advanced land surface–hydrology model with the Penn State–NCAR MM5 modeling system. Part I: Model implementation and sensitivity, Monthly weather review, 129, 569-585, 2001.

Chou, M.-D. and Suarez, M. J.: An efficient thermal infrared radiation parameterization for use in general circulation models, 1994.

Donahue, N., Robinson, A., Stanier, C., and Pandis, S.: Coupled partitioning, dilution, and chemical aging of semivolatile organics, Environmental science & technology, 40, 2635-2643, 2006.

EPA, U. S.: Guidance on the Use of Models and Other Analyses in Attainment Demonstrations for the 8-hour Ozone NAAQS, EPA-454/R-405-002, 2005.

EPA, U. S.: Guidance on the Use of Models and Other Analyses for Demonstrating Attainment of Air Quality Goals for Ozone, PM2:5, and Regional Haze, EPA-454/B-407-002, 2007.

Gao, C. Y., Tsigaridis, K., and Bauer, S. E.: MATRIX-VBS (v1.0): implementing an evolving organic aerosol volatility in an aerosol microphysics model, Geoscientific Model Development, 10, 751-764, 2017.

Gao, J., Zhu, B., Xiao, H., Kang, H., Pan, C., Wang, D., and Wang, H.: Effects of black carbon and boundary layer interaction on surface ozone in Nanjing, China, Atmospheric Chemistry and Physics, 18, 7081-7094, 2018.

Gao, M., Carmichael, G. R., Wang, Y., Ji, D., Liu, Z., and Wang, Z.: Improving simulations of sulfate aerosols during winter haze over Northern China: the impacts of heterogeneous oxidation by NO_2, Frontiers of Environmental Science & Engineering, 10, 2016.

Ghan, S., Laulainen, N., Easter, R., Wagener, R., Nemesure, S., Chapman, E., Zhang, Y., and Leung, R.: Evaluation of aerosol direct radiative forcing in MIRAGE, Journal of Geophysical Research: Atmospheres, 106, 5295-5316, 2001.

Gong, S. L., Barrie, L. A., J.-P. Blanchet, Salzen, K. v., U. Lohmann, and Lesins, G.: Canadian Aerosol Module: A size-segregated simulation of atmospheric aerosol processes for climate and air quality models 1. Module development, Journal of Geophysical Research, 108, 2003.

Grell, G. and Baklanov, A.: Integrated modeling for forecasting weather and air quality: A call for fully coupled approaches, Atmospheric Environment, 45, 6845-6851, 2011.

Grell, G. A.: Prognostic evaluation of assumptions used by cumulus parameterizations, Monthly weather review, 121, 764-787, 1993.

Grell, G. A., Peckham, S. E., Schmitz, R., McKeen, S. A., Frost, G., Skamarock, W. C., and Eder, B.: Fully coupled "online" chemistry within the WRF model, Atmospheric Environment, 39, 6957-6975, 2005.

Guenther, C.: Estimates of global terrestrial isoprene emissions using MEGAN (Model of Emissions of Gases and Aerosols from Nature), Atmospheric Chemistry and Physics, 6, 2006.

Heald, C. L., Jacob, D. J., Park, R. J., Russell, L. M., Huebert, B. J., Seinfeld, J. H., Liao, H., and Weber, R. J.: A large organic aerosol source in the free troposphere missing from current models, Geophysical Research Letters, 32, 2005.

Hicks, B. B., Saylor, R. D., and Baker, B. D.: Dry deposition of particles to canopies-A look back and the road forward, Journal of Geophysical Research: Atmospheres, 121, 14,691-614,707, 2016.

Hu, J., Chen, J., Ying, Q., and Zhang, H.: One-year simulation of ozone and particulate matter in China using WRF/CMAQ

https://doi.org/10.5194/gmd-2020-181
Preprint. Discussion started: 3 July 2020

490 modeling system, 1foldr Import 2019-10-08 Batch 1, 2016.

Jacob, D. J.: Heterogeneous chemistry and tropospheric ozone, Atmospheric Environment, 34, 2131-2159, 2000.

Jacobson, M. Z., Tabazadeh, A., and Turco, R. P.: Simulating equilibrium within aerosols and nonequilibrium between gases and aerosols, Journal of Geophysical Research: Atmospheres, 101, 9079-9091, 1996.

Janjić, Z. I.: The step-mountain eta coordinate model: Further developments of the convection, viscous sublayer, and
495 turbulence closure schemes, Monthly weather review, 122, 927-945, 1994.

Kouznetsov, R. and Sofiev, M.: A methodology for evaluation of vertical dispersion and dry deposition of atmospheric aerosols, Journal of Geophysical Research: Atmospheres, 117, 2012.

Langkamp, T. and Böhner, J.: Influence of the compiler on multi-CPU performance of WRFv3, Geoscientific Model Development, 4, 611-623, 2011.

500 Li, M., Zhang, Q., Kurokawa, J.-i., Woo, J.-H., He, K., Lu, Z., Ohara, T., Song, Y., Streets, D. G., and Carmichael, G. R.: MIX: a mosaic Asian anthropogenic emission inventory under the international collaboration framework of the MICS-Asia and HTAP, Atmospheric Chemistry and Physics (Online), 17, 2017.

Li, W., Zhou, S., Wang, X., Xu, Z., Yuan, C., Yu, Y., Zhang, Q., and Wang, W.: Integrated evaluation of aerosols from regional brown hazes over northern China in winter: Concentrations, sources, transformation, and mixing states, Journal
505 of Geophysical Research: Atmospheres, 116, 2011.

Lin, H., Feng, X., Fu, T.-M., Tian, H., Ma, Y., Zhang, L., Jacob, D. J., Yantosca, R. M., Sulprizio, M. P., and Lundgren, E. W.: WRF-GC: Online coupling of WRF and GEOS-Chem for regional atmospheric chemistry modeling, Part 1: Description of the one-way model (v1. 0), Geosci. Model Dev. Discuss, 2020, 1-39, 2020.

Lin, Y.-L., Farley, R. D., and Orville, H. D.: Bulk parameterization of the snow field in a cloud model, Journal of climate
510 and applied meteorology, 22, 1065-1092, 1983.

Liu, S., McKeen, S., Hsie, E. Y., Lin, X., Kelly, K., Bradshaw, J., Sandholm, S., Browell, E., Gregory, G., and Sachse, G.: Model study of tropospheric trace species distributions during PEM-West A, Journal of Geophysical Research: Atmospheres, 101, 2073-2085, 1996.

Lu, X., Zhang, L., Wu, T., Long, M. S., Wang, J., Jacob, D. J., Zhang, F., Zhang, J., Eastham, S. D., and Hu, L.: Development
515 of the global atmospheric general circulation-chemistry model BCC-GEOS-Chem v1. 0: model description and evaluation, Geosci. Model Dev. Discuss., 2020.

Marticorena, B. and Bergametti, G.: Modeling the atmospheric dust cycle: 1. Design of a soil-derived dust emission scheme, Journal of geophysical research: atmospheres, 100, 16415-16430, 1995.

Michel, A., Usher, C., and Grassian, V.: Reactive uptake of ozone on mineral oxides and mineral dusts, Atmospheric
520 Environment, 37, 3201-3211, 2003.

Mlawer, E. J., Taubman, S. J., Brown, P. D., Iacono, M. J., and Clough, S. A.: Radiative transfer for inhomogeneous atmospheres: RRTM, a validated correlated-k model for the longwave, Journal of Geophysical Research: Atmospheres, 102, 16663-16682, 1997.

Morris, R. E., McNally, D. E., Tesche, T. W., Tonnesen, G., Boylan, J. W., and Brewer, P.: Preliminary Evaluation of the
525 Community Multiscale Air Quality Model for 2002 over the Southeastern United States, Journal of the Air & Waste Management Association, 55, 1694-1708, 2005.

Petroff, A. and Zhang, L.: Development and validation of a size-resolved particle dry deposition scheme for application in aerosol transport models, Geoscientific Model Development, 3, 753-769, 2010.

Phadnis, M. J. and Carmichael, G. R.: Numerical investigation of the influence of mineral dust on the tropospheric
530 chemistry of East Asia, Journal of Atmospheric Chemistry, 36, 285-323, 2000.

Seinfeld, J. H. and Pandis, S. N.: Atmospheric chemistry and physics: from air pollution to climate change, John Wiley & Sons, 2012.

Seisel, S., Börensen, C., Vogt, R., and Zellner, R.: The heterogeneous reaction of HNO_3 on mineral dust and γ-alumina

https://doi.org/10.5194/gmd-2020-181
Preprint. Discussion started: 3 July 2020

surfaces: a combined Knudsen cell and DRIFTS study, Physical Chemistry Chemical Physics, 6, 5498-5508, 2004.

Skamarock, W. C., Klemp, J. B., Dudhia, J., Gill, D. O., Barker, D. M., Wang, W., and Powers, J. G.: A description of the Advanced Research WRF version 3, National Center for Atmospheric Research Technical note, NCAR/TN-475+STR, 113pp, 2008.

Spracklen, D., Jimenez, J., Carslaw, K., Worsnop, D., Evans, M., Mann, G., Zhang, Q., Canagaratna, M., Allan, J., and Coe, H.: Aerosol mass spectrometer constraint on the global secondary organic aerosol budget, Atmospheric Chemistry and Physics, 11, 12109-12136, 2011.

Tsinghua University, 2006. Control Strategy and Measurement of PM_{10} and O_3 Pollution in Beijing City. Report to Beijng Environmental Protection Bureau, Beijing, China (in Chinese).

Wang, H., Xue, M., Zhang, X. Y., Liu, H. L., Zhou, C. H., Tan, S. C., Che, H. Z., Chen, B., and Li, T.: Mesoscale modeling study of the interactions between aerosols and PBL meteorology during a haze episode in Jing–Jin–Ji (China) and its nearby surrounding region – Part 1: Aerosol distributions and meteorological features, Atmospheric Chemistry and Physics, 15, 3257-3275, 2015a.

Wang, K., Zhang, Y., Nenes, A., and Fountoukis, C.: Implementation of dust emission and chemistry into the Community Multiscale Air Quality modeling system and initial application to an Asian dust storm episode, Atmospheric Chemistry and Physics, 12, 10209-10237, 2012.

Wang, K., Zhang, Y., Yahya, K., Wu, S.-Y., and Grell, G.: Implementation and initial application of new chemistry-aerosol options in WRF/Chem for simulating secondary organic aerosols and aerosol indirect effects for regional air quality, Atmospheric Environment, 115, 716-732, 2015b.

Wang, L., Jang, C., Zhang, Y., Wang, K., Zhang, Q., Streets, D., Fu, J., Lei, Y., Schreifels, J., and He, K.: Assessment of air quality benefits from national air pollution control policies in China. Part II: Evaluation of air quality predictions and air quality benefits assessment, Atmospheric Environment, 44, 3449-3457, 2010.

Wang, X., Wang, H., Xue, L., Wang, T., Wang, L., Gu, R., Wang, W., Tham, Y. J., Wang, Z., Yang, L., Chen, J., and Wang, W.: Observations of N_2O_5 and $ClNO_2$ at a polluted urban surface site in North China: High N_2O_5 uptake coefficients and low $ClNO_2$ product yields, Atmospheric Environment, 156, 125-134, 2017.

Wang, Y., Zhuang, G., Sun, Y., and An, Z.: The variation of characteristics and formation mechanisms of aerosols in dust, haze, and clear days in Beijing, Atmospheric Environment, 40, 6579-6591, 2006.

Wong, D. C., Pleim, J., Mathur, R., Binkowski, F., Otte, T., Gilliam, R., Pouliot, G., Xiu, A., Young, J. O., and Kang, D.: WRF-CMAQ two-way coupled system with aerosol feedback: software development and preliminary results, Geoscientific Model Development, 5, 299-312, 2012.

Wu, M., Liu, X., Zhang, L., Wu, C., Lu, Z., Ma, P.-L., Wang, H., Tilmes, S., Mahowald, N., Matsui, H., and Easter, R. C.: Impacts of Aerosol Dry Deposition on Black Carbon Spatial Distributions and Radiative Effects in the Community Atmosphere Model CAM5, Journal of Advances in Modeling Earth Systems, 10, 1150–1171, 2018.

Zhang, J. and Shao, Y.: A new parameterization of particle dry deposition over rough surfaces, Atmos. Chem. Phys, 14, 12429-12440, 2014.

Zhang, L., Gong, S., Padro, J., and Barrie, L.: A size-segregated particle dry deposition scheme for an atmospheric aerosol module, Atmospheric Environment, 35, 549-560, 2001.

Zhang, L., Guo, X., Zhao, T., Gong, S., Xu, X., Li, Y., Luo, L., Gui, K., Wang, H., Zheng, Y., and Yin, X.: A modelling study of the terrain effects on haze pollution in the Sichuan Basin, Atmospheric Environment, 196, 77-85, 2019.

Zhang, L. and He, Z.: Technical Note: An empirical algorithm estimating dry deposition velocity of fine, coarse and giant particles, Atmospheric Chemistry and Physics, 14, 3729-3737, 2014.

Zhang, Y. and Carmichael, G. R.: The role of mineral aerosol in tropospheric chemistry in East Asia—A model study, Journal of Applied Meteorology, 38, 353-366, 1999.

Zhang, Y., Pan, Y., Wang, K., Fast, J. D., and Grell, G. A.: WRF/Chem-MADRID: Incorporation of an aerosol module into

https://doi.org/10.5194/gmd-2020-181
Preprint. Discussion started: 3 July 2020

WRF/Chem and its initial application to the TexAQS2000 episode, Journal of Geophysical Research, 115, 2010.

Zhao, X., Zhao, P., Xu, J., Meng, W., Pu, W., Dong, F., He, D., and Shi, Q.: Analysis of a winter regional haze event and its formation mechanism in the North China Plain, Atmospheric Chemistry & Physics Discussions, 13, 2013.

Zheng, B., Zhang, Q., Zhang, Y., He, K. B., Wang, K., Zheng, G. J., Duan, F. K., Ma, Y. L., and Kimoto, T.: Heterogeneous chemistry: a mechanism missing in current models to explain secondary inorganic aerosol formation during the January 2013 haze episode in North China, Atmospheric Chemistry and Physics, 15, 2031-2049, 2015.

Zhou, C.-H., Gong, S., Zhang, X.-Y., Liu, H.-L., Xue, M., Cao, G.-L., An, X.-Q., Che, H.-Z., Zhang, Y.-M., and Niu, T.: Towards the improvements of simulating the chemical and optical properties of Chinese aerosols using an online coupled model – CUACE/Aero, Tellus B, 64, 2012.

Zhou, Y., Zhao, Y., Mao, P., Zhang, Q., Zhang, J., Qiu, L., and Yang, Y.: Development of a high-resolution emission inventory and its evaluation and application through air quality modeling for Jiangsu Province, China, Atmospheric Chemistry and Physics, 17, 211-233, 2017.

https://doi.org/10.5194/gmd-2020-181
Preprint. Discussion started: 3 July 2020

Geoscientific Model Development Discussions
Open Access
EGU

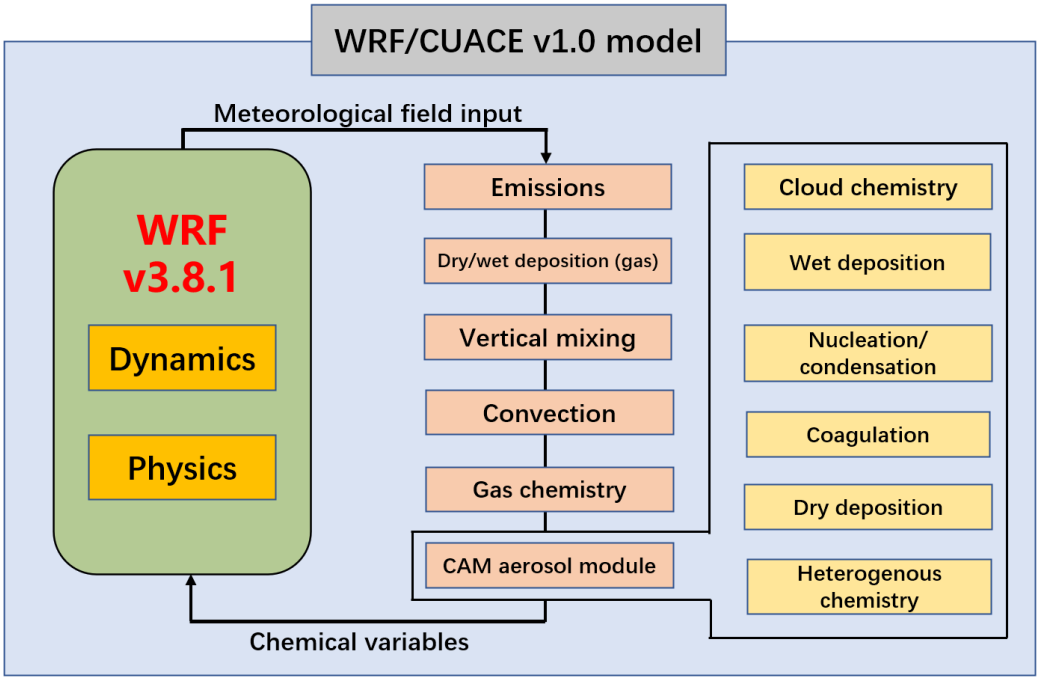

Figure 1. Schematic of modules in the WRF/CUACE v1.0 system.

https://doi.org/10.5194/gmd-2020-181
Preprint. Discussion started: 3 July 2020

Geoscientific Model Development
Discussions
Open Access
EGU

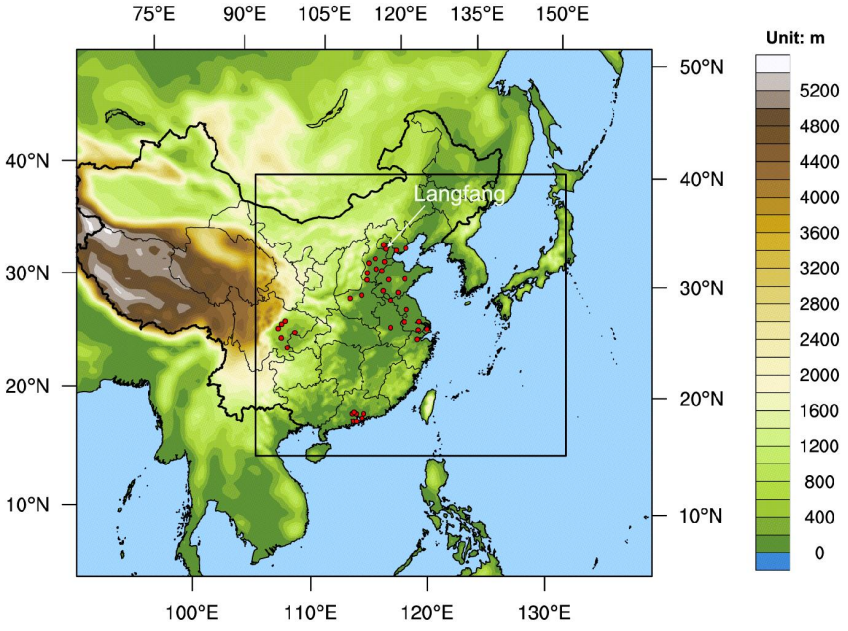

595 **Figure 2. Model domains with the terrain distribution. Red circles indicate the cities where the surface observations of air pollutants are used for model evaluation, and Langfang indicates that a nearby station (Xianghe site) conducted intensive SIA observation during January 2019.**

https://doi.org/10.5194/gmd-2020-181
Preprint. Discussion started: 3 July 2020

Geoscientific Model Development
Discussions
Open Access
EGU

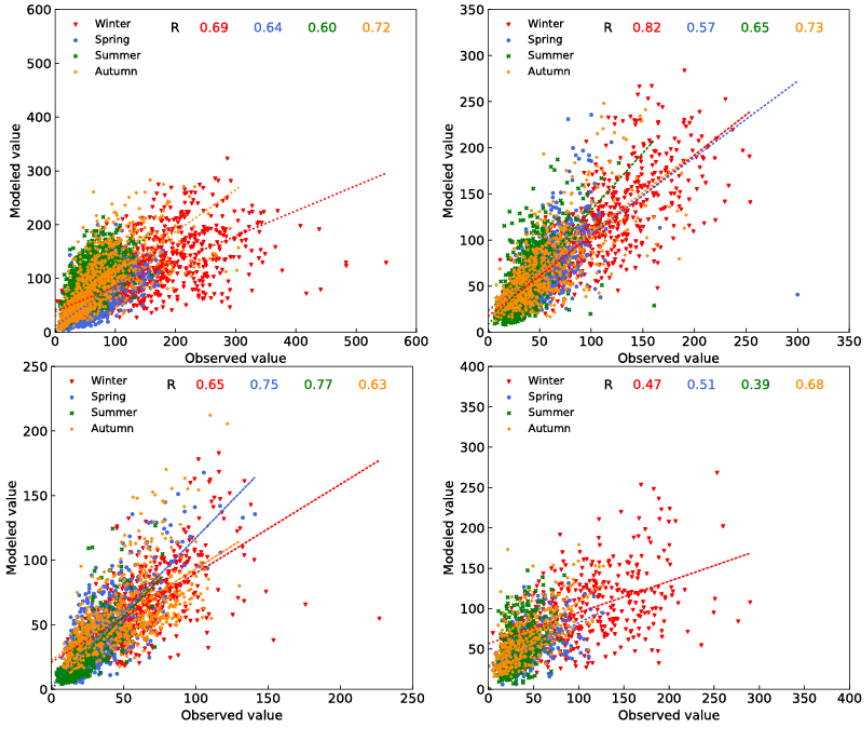

Figure 3. Scatter plots and correlation coefficients of daily $PM_{2.5}$ concentrations (ug m−3) between observed and simulated values in different seasons in the (a) NCP, (b) YRD, (c) PRD, and (d) SCB regions.

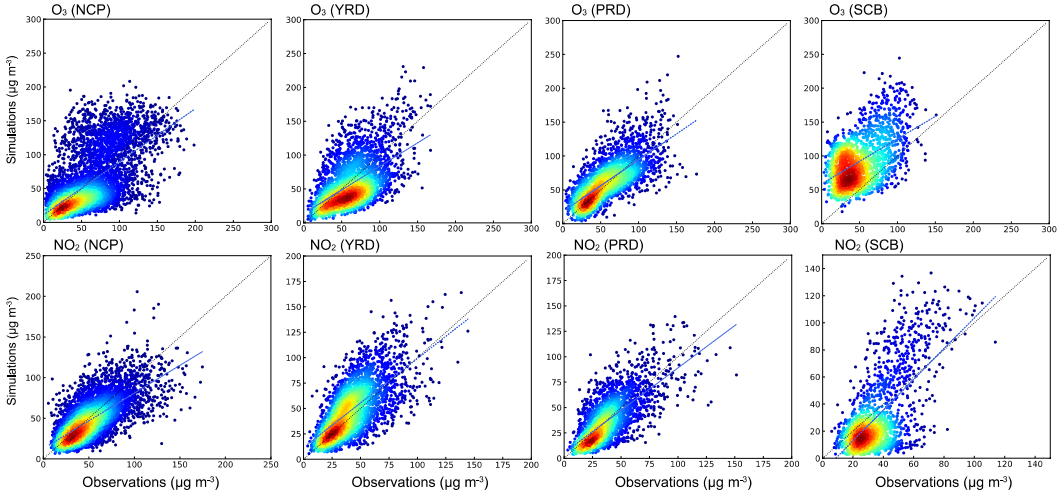

Figure 4. Scatter plots of modelled and observed hourly concentrations of O_3 and NO_2 in the NCP, YRD, PRD, and SCB regions.

https://doi.org/10.5194/gmd-2020-181
Preprint. Discussion started: 3 July 2020

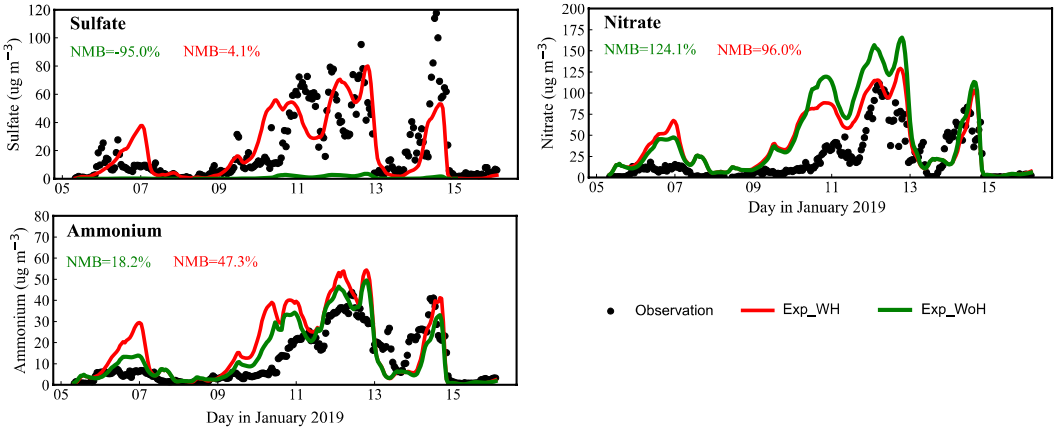

Figure 5. Observed and simulated hourly SIA concentrations from the Exp_WH and Exp_WoH experiments at the Langfang site.

610

https://doi.org/10.5194/gmd-2020-181
Preprint. Discussion started: 3 July 2020

Geoscientific Model Development Discussions

Table 1 Uptake coefficients for reactions (14)-(22).

Gas species	Uptake coefficients	References
H_2O_2	$\gamma = 1.0 \times 10^{-4}$	Bian and Zender (2003)
HNO_3	$\gamma = 1.0 \times 10^{-1}$	Seisel et al. (2004)
HO_2	$\gamma = 1.0 \times 10^{-1}$	Phadnis and Carmichael (2000)
N_2O_5	$\gamma = \begin{cases} \gamma_{low}, RH \in [0,50\%] \\ \gamma_{low} + (\gamma_{high} - \gamma_{low})/(RH_{max} \\ \times (RH - 0.5), RH \in (50\%, RH_{max} \\ \gamma_{high}, RH \in (RH_{max}\{ \end{cases}$	Wang et al. (2012)
NO_2		Zheng et al. (2015)
NO_3		
O_3	$\gamma = 3.0 \times 10^{-5}$	Michel et al. (2003)
OH	$\gamma = 1.0 \times 10^{-4}$	Zhang and Carmichael (1999)
SO_2	$\gamma = \begin{cases} \gamma_{low}, RH \in [0,50\%] \\ \gamma_{low} + (\gamma_{high} - \gamma_{low})/(RH_{max} \\ \times (RH - 0.5), RH \in (50\%, RH_{max} \\ \gamma_{high}, RH \in (RH_{max}\{ \end{cases}$	Zheng et al. (2015)

615 **Table 2 Physical parameterization schemes used in the modelling study.**

Physical management	Parameterization	References
Microphysics scheme	Lin	Lin et al. (1983)
Shortwave radiation	Goddard	Chou and Suarez (1994)
Longwage radiation	RRTM	Mlawer et al. (1997)
Land surface scheme	Noah	Chen and Dudhia (2001)
Boundary layer scheme	MYJ	Janjić (1994)
Cumulus scheme	Grell-3D	Grell (1993)

https://doi.org/10.5194/gmd-2020-181
Preprint. Discussion started: 3 July 2020

Geoscientific Model Development Discussions

Table 3 Statistical metrics for $PM_{2.5}$ in four haze contaminated areas (2013–2017), in which bold, normal , and italic font for MFB and MFE correspond to the "excellent", "good", and "average" levels in Morris et al. (2005), respectively.

	R	MB	ME	NMB	NME	MFB	MFE
		μg m^{-3}	μg m^{-3}	%	%	%	%
NCP	0.59	-5.0	44.5	-5.4	47.5	3.3	49.1
Winter	0.59	-45.0	67.7	-28.4	42.7	-22.5	47.0
Spring	0.57	-9.5	28.0	-14.0	41.1	-20.7	47.4
Summer	0.47	33.9	42.9	55.1	69.8	*44.9*	*56.3*
Autumn	0.63	-0.8	39.2	-0.9	45.4	9.0	45.9
YRD	0.71	12.9	26.9	21.8	45.3	21.1	42.9
Winter	0.75	6.0	30.6	6.4	32.5	**8.5**	**34.1**
Spring	0.49	14.2	26.3	25.4	47.1	19.1	40.0
Summer	0.56	16.4	23.3	47.8	67.9	26.7	49.4
Autumn	0.66	15.1	27.3	28.7	51.8	29.5	48.0
PRD	0.68	5.3	17.1	13.1	42.1	8.6	40.1
Winter	0.56	3.0	20.5	5.0	34.6	**5.5**	**34.4**
Spring	0.64	6.9	17.6	19.5	49.7	4.2	45.6
Summer	0.68	2.8	8.5	14.8	44.4	5.9	39.0
Autumn	0.54	8.6	21.8	17.7	45.2	18.3	41.9
SCB	0.59	7.6	31.3	12.2	50.3	*20.7*	*51.4*
Winter	0.41	-13.3	46.7	-11.5	40.4	-8.3	45.2
Spring	0.49	4.1	22.4	8.4	45.9	11.4	46.1
Summer	0.40	21.6	28.2	60.4	78.6	*38.7*	*58.9*
Autumn	0.58	15.9	28.2	31.4	55.7	*37.2*	*54.3*

https://doi.org/10.5194/gmd-2020-181
Preprint. Discussion started: 3 July 2020

Geoscientific Model Development Discussions

Table 4 Statistical metrics for O_3 and NO_2 concentrations. Criteria for O_3 are from the EPA (2005, 2007). The values that do not meet the criteria are in bold.

Variables		NCP	YRD	PRD	SCB	Criteria
O_3	R	0.64	0.66	0.77	0.60	
	NMB (%)	-0.60	-8.21	7.24	**77.61**	$\leqslant \pm 15$
	IOA	0.80	0.80	0.87	0.67	
NO_2	R	0.60	0.64	0.67	0.57	
	NMB (%)	-6.62	14.42	-2.45	-14.36	
	IOA	0.77	0.77	0.81	0.71	

625